

**Article: 2013-032**

**Article-type: research-article**

**Subject: Research Article**

## **Specific Queries (see AQ? in margins)**

No	Query
1	Please check this proof carefully for errors, once it is published online no further changes can be made. In particular, check that figures, tables and equations are correct.

## Messinian productivity changes in the northeastern Atlantic and their relationship to the closure of the Atlantic–Mediterranean gateway: implications for Neogene palaeoclimate and palaeoceanography

JOSÉ N. PÉREZ-ASENSIO<sup>1,2\*</sup>, JULIO AGUIRRE<sup>1</sup>, GERHARD SCHMIEDL<sup>3</sup> & JORGE CIVIS<sup>4</sup>

<sup>1</sup>*Departamento de Estratigrafía y Paleontología, Facultad de Ciencias, Universidad de Granada, Avenida Fuentenueva s.n., 18002 Granada, Spain*

<sup>2</sup>*Present address: Earth and Environmental Science Section, University of Geneva, Rue des Maraîchers 13, 1205, Geneva, Switzerland*

<sup>3</sup>*Center for Earth System Research and Sustainability, University of Hamburg, Bundesstraße 55, 20146 Hamburg, Germany*

<sup>4</sup>*Instituto Geológico y Minero de España, Ríos Rosas 23, 28003 Madrid, Spain*

\*Corresponding author (e-mail: [Noel.PerezAsensio@unige.ch](mailto:Noel.PerezAsensio@unige.ch))

**Abstract:** The stable isotope composition of planktic and benthic foraminifera and the distribution of selected benthic foraminiferal species from a Messinian record of the lower Guadalquivir Basin, northeastern Atlantic Ocean, show that regional productivity changes were linked to glacioeustatic fluctuations. Glacial periods were characterized by poorly ventilated bottom waters as a result of weak Atlantic Meridional Overturning Circulation (AMOC), and by phases of high productivity related to intensified upwelling. In contrast, well-ventilated bottom waters owing to strong AMOC, the presence of degraded organic matter in the upper slope, and high input of degraded terrestrial organic matter derived from fluvial discharge to the outer shelf were recorded during interglacial periods. Before closure of the adjacent Guadalhorce Corridor at 6.18 Ma, which was the final active Betic Atlantic–Mediterranean gateway, the study area was alternately influenced by well-ventilated Mediterranean Outflow Water (MOW) and poorly ventilated Atlantic Upwelled Water (AUW). Following closure of the corridor, cessation of the MOW reduced the AMOC and promoted glacial conditions in the northern hemisphere, resulting in the establishment of local upwelling cells.

The dynamics of past global climate changes are intimately related to the exchange of CO<sub>2</sub> between atmosphere and ocean, and feedbacks involving the marine biological pump and organic carbon cycling. Changes in the production, sequestration and remineralization of marine organic matter during glacial–interglacial cycles are closely linked to global thermohaline circulation and the distribution and intensity of upwelling systems (Sarmiento & Toggweiler 1984; Lyle *et al.* 1992).

At present, regions under upwelling influence are those with the highest primary productivities in the world ocean (Bakun *et al.* 2010). In the Atlantic Ocean, the main upwelling areas are located in its eastern parts, mainly along the West African coast and the Iberian Peninsula, and are driven by prevailing wind systems (Schmiedl *et al.* 1997; Martinez *et al.* 1999; Bakun *et al.* 2010). The intensity and extent of upwelling currents are commonly controlled by Ekman pumping, which in the northern hemisphere is the vertical spiral movement of bottom waters induced by strong northerly trade winds and the Coriolis force (Tomczak & Godfrey 1994; Lebreiro *et al.* 1997; Smyth *et al.* 2001).

The intensity of upwelling systems has changed with glacial–interglacial climate oscillations and the associated eustatic sea-level fluctuations and meridional temperature gradients. Thus, upwelling was more intense during glacial periods owing to strong wind stress (Lebreiro *et al.* 1997; Martinez *et al.* 1999; Salgueiro *et al.* 2010). Global palaeo-circulation patterns also influenced productivity related to upwelling. During glacial periods, the Atlantic Meridional Overturning Circulation (AMOC) was reduced (Broecker *et al.* 1985). Furthermore, large influxes of freshwater released in the North Atlantic decreased net water density and led to the collapse of the AMOC (McManus *et al.* 2004; Rogerson

*et al.* 2010). Subsequently, in the early stages of interglacial periods, the intensification and shoaling of the dense Mediterranean Outflow Water (MOW) plume promoted an abrupt resumption of the AMOC (Rogerson *et al.* 2006, 2012). Furthermore, reduction or interruption of the MOW resulted in decrease or interruption of the North Atlantic Deep Water formation (Rahmstorf 1998). As a result, the AMOC reduced and diminished poleward heat transport in the Atlantic, leading to cooling and ice sheet growth in the northern hemisphere (Zahn *et al.* 1997; Clark *et al.* 2002; McManus *et al.* 2004). This glaciation in turn promoted high-productivity conditions owing to stronger winds that induced Ekman pumping, once again stimulating upwelling and increased Atlantic Upwelled Water (AUW) influence in the NE Atlantic (Lebreiro *et al.* 1997; Zahn *et al.* 1997; Clark *et al.* 2002; Salgueiro *et al.* 2010).

In addition to primary productivity, organic matter in marine settings can be delivered as terrestrial input from rivers that discharge onto coastal shelves (McKee *et al.* 2004). A high supply of terrestrial organic matter can provide an important food resource for marine benthic ecosystems, and its degradation may result in oxygen depletion of the bottom and pore waters (van der Zwaan & Jorissen 1991; Jorissen *et al.* 1992; Donnici & Serandrei-Barbero 2002). Inner-shelf areas close to river mouths are excellent examples of high productivity localized by freshwater discharge, rich in nutrients and suspended terrestrial organic particles. High riverine discharge occurs during periods of intense rainfall, as at the Rhône and Tagus prodeltas, and the continental shelf of the Gulf of Cádiz, which is affected by the Guadalquivir River (Cabeçadas & Brogueira 1997; Lebreiro *et al.* 2006; Villanueva-Guimerans & Canudo 2008; Rodrigues *et al.* 2009; Goineau *et al.* 2011; Anfuso *et al.* 2013). Periods of intense riverine discharge are more frequent

1  
2  
3  
4  
5  
6  
7  
8  
9  
10  
11  
12  
13  
14  
15  
16  
17  
18  
19  
20  
21  
22  
23  
24  
25  
26  
27  
28  
29  
30  
31  
32  
33  
34  
35  
36  
37  
38  
39  
40  
41  
42  
43  
44  
45  
46  
47  
48  
49  
50  
51  
52  
53  
54  
55  
56  
57  
58  
59  
60  
61  
62  
63  
64

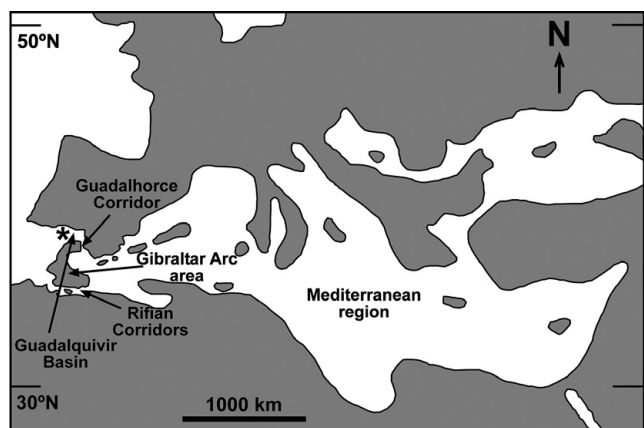


**Fig. 1.** Palaeogeography of the Guadalquivir Basin, Gibraltar Arc area, and the Mediterranean region during the early Messinian (based on Braga *et al.* 2009; Martín *et al.* 2009). Asterisk marks the location of the Montemayor-1 core.

during warmer, relatively more humid, interglacial periods (Frei *et al.* 1998).

Biogeochemical cycles are also influenced by the opening and closure of oceanic gateways (e.g. Schneider & Schmittner 2006), as these palaeogeographical changes affected palaeo-circulation patterns. One of these was the temporary closure of Atlantic–Mediterranean connections during the late Messinian (Riding *et al.* 1998; Krijgsman *et al.* 1999; Pérez-Asensio *et al.* 2013). The interaction of this geological event with Atlantic circulation and glacio-eustatic sea-level changes is becoming better understood (e.g. Pérez-Asensio *et al.* 2012a; Rogerson *et al.* 2012), but little detailed analysis of its consequences for marine nutrient cycling and potential climate feedbacks has previously been undertaken. In the North Atlantic, cessation of the Mediterranean Outflow Water owing to the Messinian closure of the Betic gateways interrupted North Atlantic Deep Water production and weakened the AMOC, leading to cooling in the northern hemisphere (Pérez-Asensio *et al.* 2012a). Coincidentally, small- or medium-scale glaciations with limited ice sheets developed in the northern hemisphere at about 7–6 Ma (Fronval & Jansen 1996; Thiede *et al.* 1998). This cooling would have reduced surface water temperatures in the North Atlantic, thereby enhancing coast-parallel trade winds that promoted upwelling currents and high productivity (Hughen *et al.* 1996; Clark *et al.* 2002). Results inferred from modelling also suggest intense winds during the Messinian (Murphy *et al.* 2009), but there have been no previous studies of the relationship between productivity changes in the northeastern Atlantic and global climate and oceanography to validate these hypotheses.

Proxies that can be used to estimate palaeoproductivity changes include the relative abundance of benthic foraminifera, diatoms, radiolarians, fish debris, phosphorite grains, and stable C isotopes. In this study, foraminiferal stable oxygen and carbon isotope records and the distribution of selected benthic foraminiferal species have been analysed from the Montemayor-1 borehole (SW Spain, Fig. 1). This core is located in the Guadalquivir Basin, an open marine embayment that constituted the Atlantic side of the Guadalhorce Corridor, the final Betic Atlantic–Mediterranean gateway, and that closed at 6.18 Ma (Martín *et al.* 2001, 2009; Pérez-Asensio *et al.* 2012a). According to benthic foraminiferal assemblages, the Messinian record of the Montemayor-1 core represents a shallowing-upward sequence from middle- and upper-slope to shelf-edge and finally outer-shelf deposits (Pérez-Asensio *et al.* 2012b; Fig. 2).

The middle-slope and part of the upper-slope sediments deposited prior to closure of the Guadalhorce seaway were under the influence of the MOW (Pérez-Asensio *et al.* 2012a). The remainder of the upper-slope sediments, the shelf-edge and outer-shelf deposits are younger than 6.18 Ma and were not affected by the MOW. Palaeoceanographical changes produced by the MOW interruption affected the AMOC and climate, leading to cooling in the northern hemisphere (Pérez-Asensio *et al.* 2012a). The location of this core is therefore ideal to (1) investigate productivity changes and organic carbon cycling in the eastern North Atlantic during the Messinian, (2) assess effects of cessation of the MOW on palaeoproductivity, and (3) decipher relationships between Neogene productivity and global oceanography and climate.

### Geographical and geological setting

The study area is located in the northwestern margin of the lower Guadalquivir Basin (SW Spain), an ENE–WSW-elongated Atlantic foreland basin that is bounded to the north by the Iberian Massif, to the south by the Betic Cordillera, and to the west by the Atlantic Ocean (Sanz de Galdeano & Vera 1992; Vera 2000; Braga *et al.* 2002). The sedimentary fill of the basin consists of marine deposits ranging from early Tortonian to late Pliocene (Aguirre 1992, 1995; Aguirre *et al.* 1995; Ríaza & Martínez del Olmo 1996; Sierro *et al.* 1996).

The Guadalquivir Basin acted as a corridor, the ‘North Betic Strait’, connecting the Atlantic and the Mediterranean during the early Tortonian (Aguirre *et al.* 2007; Martín *et al.* 2009; Braga *et al.* 2010). Betic seaways that connected the Atlantic and the Mediterranean through the Guadalquivir Basin were progressively closed during the late Miocene (Esteban *et al.* 1996; Martín *et al.* 2001; Braga *et al.* 2003; Betzler *et al.* 2006; Martín *et al.* 2009), culminating in the closure of the Guadalhorce Corridor in the early Messinian (Martín *et al.* 2001; Pérez-Asensio *et al.* 2012a). Following its closure, the only remaining Atlantic–Mediterranean connections were through the Rifian Corridors in northern Morocco (Esteban *et al.* 1996).

Neogene deposits of the lower Guadalquivir Basin in the study area have been divided into four lithostratigraphic units formally described as formations. From bottom to top these are: (1) mixed carbonate–siliciclastic deposits of the Niebla Formation (Civis *et al.* 1987; Baceta & Pendón 1999); (2) greenish–bluish clays of the Arcillas de Gibralfón Formation (Civis *et al.* 1987); (3) fossiliferous sands and silts of the Arenas de Huelva Formation (Civis *et al.* 1987); (4) sands of the Arenas de Bonares Formation (Mayoral & Pendón 1987).

### Materials and methods

The 260 m long continuous Montemayor-1 core was drilled close to Huelva (Fig. 1). The cored sediments range from latest Tortonian to early Pliocene in age (Larrasoña *et al.* 2008; Pérez-Asensio *et al.* 2012a, 2013; Jiménez-Moreno *et al.* 2013). In this study, the 140 m interval from 240 to 100 m has been studied. It ranges from 6.67 to 5.38 Ma (Messinian) and is in marine sediments of the Arcillas de Gibralfón Formation (Fig. 3).

For faunal analyses, a total of 255 samples were collected at a sampling interval of 0.5 m. Samples were wet sieved over a 63 µm mesh and dried in an oven at 40 °C. Using a microsampler, samples were divided into subsamples containing at least 300 benthic foraminifera. Subsamples were dry-sieved over a 125 µm mesh, and the benthic foraminifera were identified and counted. The counts are expressed as percentages, representing the relative abundance of each taxon in the assemblage. To assess changes in flux,

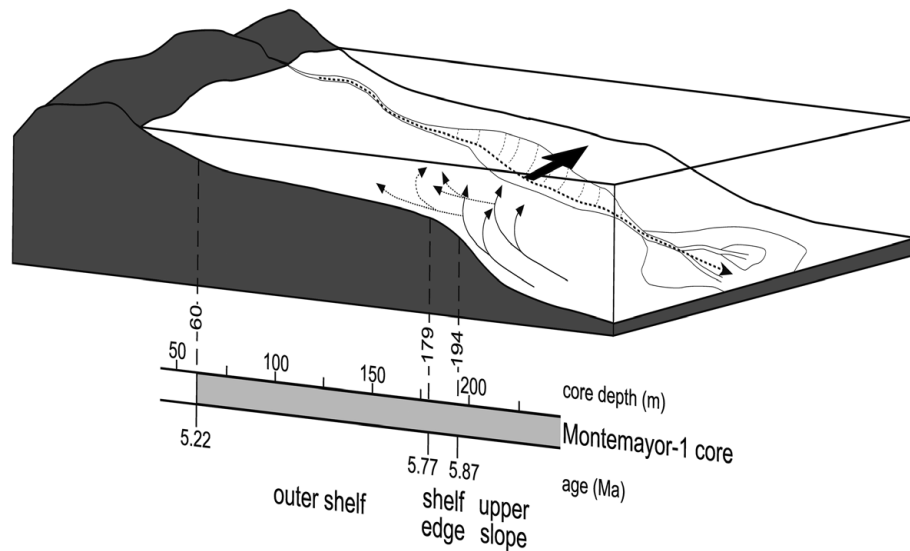


**Fig. 2.** Sketch showing the palaeoenvironments of the Montemayor-1 core during the Messinian (upper slope, shelf edge, outer shelf). The main organic matter sources are shown by fine arrows indicating upwelling currents in the upper slope, fine dashed arrows denoting upwelling currents entering the outer shelf, and bold dashed arrow representing river runoff. The wide black arrow shows superficial currents along the shelf edge (see also Fig. 7d).

provenance and degradation state of the organic matter we used the relative abundances of high-productivity target taxa including *Uvigerina peregrina s.l.* (*U. peregrina* + *U. pygmaea*), which thrives in environments with input of fresh marine organic matter, *Bulimina subulata* related to degraded marine organic matter, and *Brizalina spathulata* and *Bulimina aculeata* indicative of supply of degraded continental organic matter (Donnici & Serandrei-Barbero 2002; Schmiedl & Leuschner 2005; Murray 2006; Diz & Francés 2008; Duchemin *et al.* 2008; Schmiedl *et al.* 2010). In addition, changes in palaeo-oxygenation of the bottom water mass were analysed using the index of Schmiedl *et al.* (2003),  $[\text{HO}/(\text{HO} + \text{LO}) + \text{Div}] \times 0.5$ , in which HO is the relative abundance of high-oxygen indicators (epifaunal taxa and miliolids), LO is the relative abundance of low-oxygen indicators (deep infaunal taxa), and Div is normalized benthic foraminiferal diversity using the Shannon index (H) calculated with the software PAST (Hammer *et al.* 2001).

For stable oxygen and carbon isotope analyses, a total of 160 samples were analysed. The sampling interval was 0.5 m from 240–170 m, and 2.5 m from 170–100 m. Two analyses per sample were performed, one with about 10 individuals of *Cibicidoides pachydermus* and another with 20 individuals of *Globigerina bulloides* picked from the size fraction  $>125 \mu\text{m}$ . Prior to the analyses, diagenetic alteration was assessed by checking for dissolution and/or recrystallization of shells under the SEM at 3000 to 10000 $\times$  magnification. Any examples showing cement within skeletal pores or as overgrowths were discarded, as were any that showed evidence of dissolution. Foraminifera were cleaned with an ultrasonic bath and washed with deionized water. Samples were analysed at the Leibniz-Laboratory for Radiometric Dating and Isotope Research in Kiel (Germany), using a Finnigan MAT 251 mass spectrometer connected to a Kiel I (prototype) on-line  $\text{CO}_2$  extraction device. Results are presented in  $\delta$ -notation as per mil deviation from the Vienna Pee Dee belemnite (VPDB) standard. Analytical reproducibility monitored by repeated analyses of NBS-19 and calibrated internal laboratory  $\text{CaCO}_3$  standards was  $< \pm 0.05\text{‰}$  for  $\delta^{13}\text{C}$  and  $< \pm 0.07\text{‰}$  for  $\delta^{18}\text{O}$ .

Pearson correlation coefficients ( $p$ ) were calculated to assess the statistical correlation between O and C stable isotopes, relative abundance of target taxa, palaeo-oxygenation index and planktonic/benthonic ratio (P/B ratio), calculated as explained by Pérez-Asensio *et al.* (2012b) (Table 1). Only coefficients with a  $p$ -value  $< 0.01$  or  $< 0.05$  were considered significant.

## Results

### High-productivity target taxa and palaeo-oxygenation index

Changes in relative abundance of the four selected benthic foraminiferal species that indicate high productivity are shown in Figure 4. Both *Uvigerina peregrina s.l.* and *Bulimina subulata* show relatively high percentages from 6.67 to 5.87 Ma (Fig. 4), although some differences are evident. In this interval, *U. peregrina s.l.* displays significant minima at about 6.44 and 6.24 Ma, and maxima at 6.67 and 6.35 Ma, whereas *B. subulata* shows a slowly increasing trend with superimposed peaks and troughs (Fig. 4). In the interval from 5.87 to 5.38 Ma, the two species diminish in percentage, although in a different manner. *Uvigerina peregrina s.l.* relative abundance decreases sharply at 5.87 Ma and then remains with low average values around 10% (Fig. 4). In contrast, *Bulimina subulata* gradually decreases upwards to negligible values (Fig. 4).

The other two selected high-productivity target taxa, *Brizalina spathulata* and *Bulimina aculeata*, show increase in percentages towards the top of the studied interval that coincide with decrease in *U. peregrina s.l.* and *B. subulata* (Fig. 4). They are, however, nearly absent from the base of the studied section (6.67 Ma) to 5.87 Ma (Fig. 4).

The palaeo-oxygenation index shows relatively high values ( $> 0.8$ ) throughout the entire studied interval (Fig. 5). However, some oxygen depletion is recorded at 6.00, 5.99, 5.96, 5.91, and 5.87 Ma. After 5.87 Ma, the oxygen depletions are more severe than in the older sediments.

### Stable isotope data

The benthic oxygen isotope record as measured in *Cibicidoides pachydermus* exhibits relatively low variations with an average value of  $+1\text{‰}$  before 6.35 Ma, followed by a gradual decrease of  $1.9\text{‰}$  up to a minimum of  $-0.9\text{‰}$  that is reached by 6.18 Ma (Figs 4 and 5). In the same interval (6.67–6.18 Ma), the planktic (*Globigerina bulloides*) oxygen isotope record shows a fluctuating trend with average values between 0 and  $-1.6\text{‰}$  (Figs 4 and 5). From 6.18 Ma onwards, the planktic and benthic  $\delta^{18}\text{O}$  curves exhibit similar trends, as is indicated by the positive correlation (Table 1). In the interval from 6.18 to 5.79 Ma, both benthic and planktic average  $\delta^{18}\text{O}$  values gradually increase. They then show stepwise decrease with two drops, at 5.75 Ma and 5.52 Ma (Figs 4 and 5).

129  
130  
131  
132  
133  
134  
135  
136  
137  
138  
139  
140  
141  
142  
143  
144  
145  
146  
147  
148  
149  
150  
151  
152  
153  
154  
155  
156  
157  
158  
159  
160  
161  
162  
163  
164  
165  
166  
167  
168  
169  
170  
171  
172  
173  
174  
175  
176  
177  
178  
179  
180  
181  
182  
183  
184  
185  
186  
187  
188  
189  
190  
191  
192

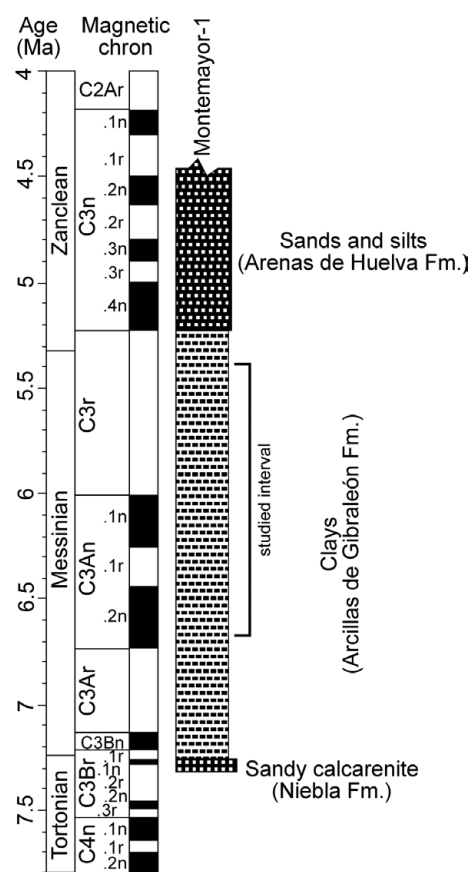


**Fig. 3.** Correlation of the lithostratigraphic formations of the Montemayor-1 core with magnetostratigraphic and geochronological time scales, highlighting the study interval. Magnetostratigraphy is based on the ATNTS2004 (Lourens *et al.* 2004) and age estimation of the deposits is based on Jiménez-Moreno *et al.* (2013).

Prior to 6.18 Ma, the benthic and planktic carbon isotope record shows a fluctuating trend with average values of +0.4‰, and -0.8‰, respectively (Figs 4 and 5). From 6.18 to 5.9 Ma, benthic and planktic  $\delta^{13}\text{C}$  values decrease by 0.8‰ and 1.3‰, respectively. In the interval from 5.9 to 5.67 Ma, the benthic  $\delta^{13}\text{C}$  values remain near +0.4‰, and the planktic  $\delta^{13}\text{C}$  values show significant relative maximum around 0‰ from 5.85 and 5.77 Ma. Finally, benthic and planktic C values gradually decrease by 0.7‰ and 1.4‰, respectively (Figs 4 and 5).

Comparing the stable isotope records with the high-productivity target taxa, high values of the benthic and planktic  $\delta^{18}\text{O}$  coincide with low benthic  $\delta^{13}\text{C}$  values, and with high abundance of *Uvigerina peregrina s.l.* and low abundance of *Bulimina subulata* (Fig. 4). In the interval between 5.67 and 5.38 Ma, low benthic and planktic  $\delta^{18}\text{O}$  values correspond to low benthic and planktic  $\delta^{13}\text{C}$  values and high percentages of *Brizalina spathulata* and *Bulimina aculeata*.

## Discussion

### *Processes influencing the stable isotope signal of foraminifera and the species composition of benthic foraminiferal faunas at continental margins*

Species associations and stable O and C isotope composition of planktic and benthic foraminifera from continental margins are influenced by a variety of global and regional processes and commonly reveal major fluctuations on glacial-to-interglacial time

scales. The glacial increases of  $\delta^{18}\text{O}$  values in both planktic and benthic foraminifera are due to the storage of the lighter  $^{16}\text{O}$  isotope in continental ice caps (Rohling & Cooke 1999, and references therein; Fig. 6a). Conversely, the delivery of  $^{16}\text{O}$  to the ocean by melting of continental ice during interglacial periods results in a lowering of marine  $\delta^{18}\text{O}$  values (Fig. 6b). During the late Miocene, this global ice effect typically accounts for *c.* 0.4–0.5‰ (Vidal *et al.* 2002). In addition, the planktic  $\delta^{18}\text{O}$  signal contains a significant temperature signal and in near-coastal settings can be additionally altered by the inflow of isotopically light freshwater through riverine runoff (Rohling & Cooke 1999; Milker *et al.* 2012).

The foraminiferal  $\delta^{13}\text{C}$  signal is influenced by a variety of processes, mainly by changes in the global C budget, the residence time of the water mass, and local processes such as removal of  $^{12}\text{C}$  by primary production and release of  $^{12}\text{C}$  by remineralization in the water column and surface sediment (Rohling & Cooke 1999; Mackensen 2008). Decrease in the global C budget during glacial periods in the Quaternary resulted in marine  $\delta^{13}\text{C}$  values 0.46–0.32‰ lower than today (Piotrowski *et al.* 2005). However, Messinian changes in global C budget might have been smaller than those during the Quaternary owing to weaker glacial–interglacial contrasts and related vegetation changes, as well as shelf exposures. In addition, an increase in the residence time of water masses, as during a slowdown of the AMOC, favoured the accumulation of  $^{12}\text{C}$ -enriched carbon dioxide from oxidized organic matter. Primary production in the photic zone preferentially extracts  $^{12}\text{C}$  from the dissolved inorganic carbon reservoir, commonly resulting in higher  $\delta^{13}\text{C}$  in the surface water (Rohling & Cooke 1999). In upwelling areas, however,  $^{13}\text{C}$ -depleted  $\text{CO}_2$ -rich subsurface waters enter the surface ocean and can result in a low  $\delta^{13}\text{C}$  signature. In deep-sea surface sediments below upwelling areas, enhanced remineralization rates of organic matter are reflected in low benthic  $\delta^{13}\text{C}$  signatures of shallow infaunal benthic foraminifera (McCorkle *et al.* 1990). Such a process accounts for low  $\delta^{13}\text{C}$  values in infaunal taxa from modern and Holocene sediments of the continental margin off NW Morocco, located beneath coastal upwelling cells (Eberwein & Mackensen 2006, 2008), and may also be expected to have operated in comparable environmental settings during the Messinian.

The microhabitat and species composition of deep-sea benthic foraminifera are principally influenced by food availability and oxygenation of bottom and pore waters, as described in the ‘TROX’ (TRotrophic OXYgen) model of Jorissen *et al.* (1995). According to this model, oligotrophic and well-ventilated ecosystems are dominated by epifaunal taxa that have little food and high-oxygen requirements. In contrast, eutrophic and low-oxygen environments are inhabited by low-diversity faunas that are dominated by deep-infaunal, low-oxygen tolerant taxa. Highest diversities and population of various microhabitats are established under mesotrophic conditions. More recent studies demonstrated that the distribution of certain taxa is additionally controlled by specific biogeochemical conditions, seasonality and quality of the supplied food. Various opportunistic species respond to input of freshly produced marine phytodetritus, whereas other species are able to feed from degraded re-suspended organic matter or from terrestrial organic matter in the vicinity of river mouths (Fontanier *et al.* 2003; Diz & Francés 2008; Duchemin *et al.* 2008; Koho *et al.* 2008).

### *Palaeoproductivity changes and organic carbon cycling in the northeastern Atlantic during the Messinian*

Changes in primary production greatly influence the interchange of dissolved inorganic carbon between oceanic and atmospheric reservoirs. Thus, sequestration of C in the oceans, or its release to

**Table 1.** Pearson correlation coefficients at  $p$ -value  $<0.01$  and  $p$ -value  $<0.05$  (in italics) of high-productivity benthic foraminiferal species, the planktic and benthic O and C isotopes, P/B ratio, and palaeo-oxygenation index

	Uvigerina peregrina s.l.	Bulimina subulata	Bulimina aculeata	Brizalina spathulata	P/B ratio	Benthic O	Benthic C	Planktic O	Planktic C	Palaeo-oxygenation index
Uvigerina peregrina s.l.	1									
Bulimina subulata		1								
Bulimina aculeata			1							
Brizalina spathulata	-0.301	-0.423	0.252	1						
P/B ratio	0.370	0.160		-0.460	1					
Benthic O	0.173	0.401		-0.211		1				
Benthic C	-0.218				0.159		1			
Planktic O		0.313			-0.199	0.376	-0.173	1		
Planktic C	-0.378	-0.198		0.349	-0.551				1	
Palaeo-oxygenation index					0.327					1

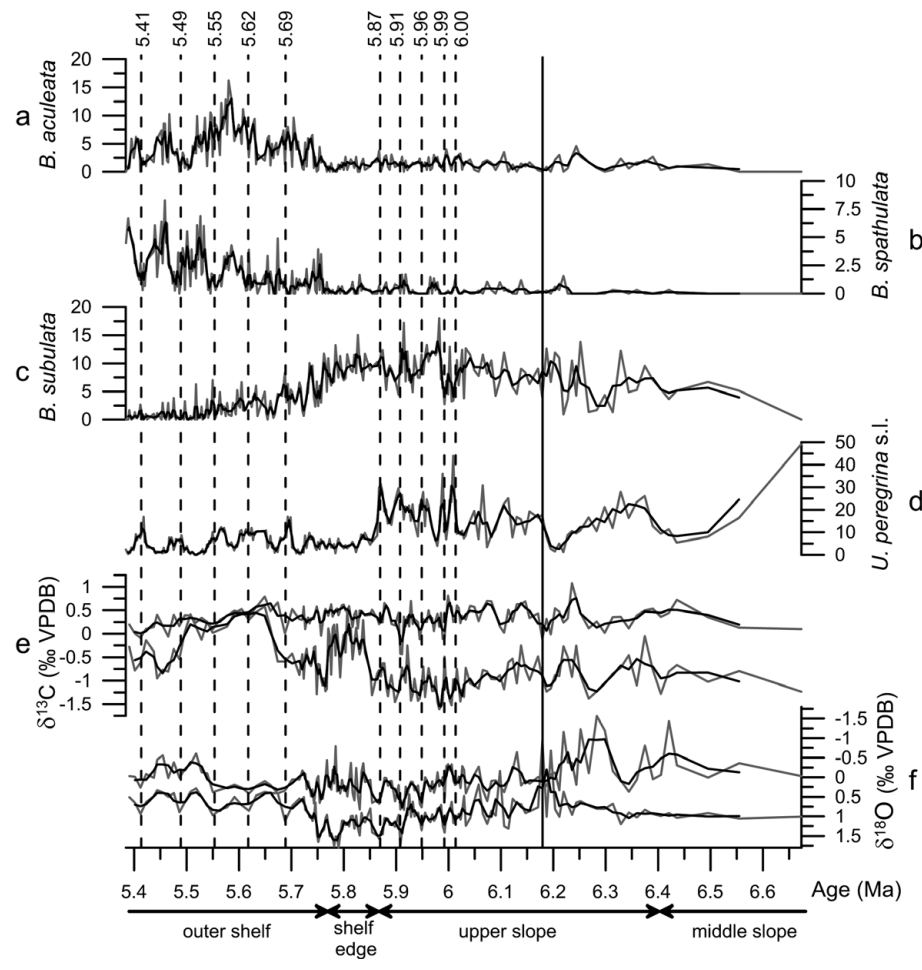


**Fig. 4.** (a) Relative abundance (%) of *Bulimina aculeata*. (b) Relative abundance (%) of *Brizalina spathulata*. (c) Relative abundance (%) of *Bulimina subulata*. (d) Relative abundance (%) of *Uvigerina peregrina s.l.* (e) Benthic (upper curve) and planktic (lower curve)  $\delta^{13}\text{C}$  records in ‰ VPDB for the Montemayor-1 core. (f) Benthic (lower curve) and planktic (upper curve)  $\delta^{18}\text{O}$  records in ‰ VPDB for the Montemayor-1 core. Black curves are the three-point running averages of the data (grey curves). The vertical dashed lines indicate 10 events of high productivity related to upwelling currents in the upper slope (6.00, 5.99, 5.96, 5.91, 5.87 Ma) and outer shelf (5.69, 5.62, 5.55, 5.49, 5.41 Ma). The vertical black continuous line at 6.18 Ma marks the end of the Atlantic-Mediterranean Betic connection through the Guadalorce Corridor. Distribution of palaeoenvironmental settings at the bottom of the figure is based on benthic foraminiferal assemblages (Pérez-Asensio *et al.* 2012b).

the atmosphere, can modify global climate. Fluctuation of sedimentary organic matter content over geological time is a dynamic balance between production, concentration and preservation, and depends upon global, regional and local factors. Accurately interpreting palaeoceanographic circulation, palaeoclimate and changes in ocean C budgets requires an understanding of how multiple factors interact to influence palaeoproductivity (e.g. sedimentation rate, sea level, ocean currents, water mass residence times, C budgets, fluvial outflow, upwelling, palaeogeography, oxygenation) and of temporal changes in organic matter supply.

In this study, the palaeo-oxygenation index is high ( $>0.8$ ) throughout the studied interval (Fig. 5). This suggests that oxygen content did not control the observed stable carbon isotope signatures and changes in benthic foraminiferal abundance, and that the presence of an oxygen minimum zone can be ruled out. Instead, our data suggest significant changes in productivity and associated organic carbon fluxes and remineralization rates in the northeastern Atlantic. These changes were linked to global glacioeustatic fluctuations and to regional palaeogeographical changes owing to the closure of the Guadalorce Corridor. Interruption of the outflow of Mediterranean

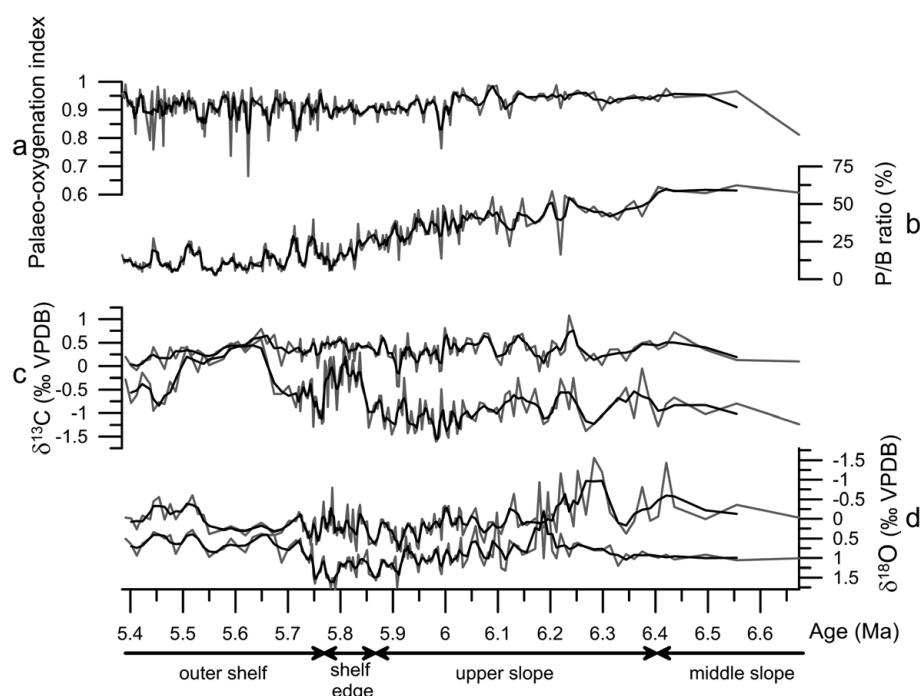


**Fig. 5.** (a) Palaeo-oxygenation index. (b) P/B ratio (%) (Pérez-Asensio *et al.* 2012b). (c) Benthic (upper curve) and planktic (lower curve)  $\delta^{13}\text{C}$  records in ‰ VPDB for the Montemayor-1 core. (d) Benthic (lower curve) and planktic (upper curve)  $\delta^{18}\text{O}$  records in ‰ VPDB for the Montemayor-1 core. Black curves are the three-point running averages of the data (grey curves). Distribution of palaeoenvironmental settings at the bottom of the figure is based on benthic foraminiferal assemblages (Pérez-Asensio *et al.* 2012b).

water after the closure of the Guadalorce Corridor at 6.18 Ma altered the thermohaline circulation in the North Atlantic and led to global cooling in the northern hemisphere (Pérez-Asensio *et al.* 2012a, 2013). Benthic foraminiferal assemblages from the Montemayor-1 core suggest a shallowing upward trend from middle–upper-slope to outer-platform settings, as noted by Pérez-Asensio *et al.* (2012b). According to those researchers, the transition from the middle–upper slope to the shelf-edge is characterized by reduction in *Anomalinoidea flintii* and *Uvigerina peregrina s.l.* and the dominance of *Planulina ariminensis*. Disappearance of the last species in the core marks the beginning of outer-shelf deposition, characterized by increased abundance of *Brizalina spathulata* and *Bulimina aculeata*. The shallowing of the depositional environment over the studied time interval is also mirrored by a decrease of the dinocyst to pollen ratio (Jiménez-Moreno *et al.* 2013).

Below, we discuss how these global, regional and local processes affected both the provenance (upwelling versus continental) and the quality (fresh or degraded) of the organic matter.

#### Upper-slope fresh and degraded organic matter linked to upwelling currents

In the upper-slope deposits of the Montemayor-1 core (from 246.5 to 194 m core depth; Fig. 2), glacial periods characterized by relatively high planktic and benthic  $\delta^{18}\text{O}$  isotopic values coincide with low benthic  $\delta^{13}\text{C}$  values (Figs 4 and 6a). This is accompanied by a weak negative correlation between planktic  $\delta^{18}\text{O}$  and benthic  $\delta^{13}\text{C}$  values (Table 1). The observed glacial drop in  $\delta^{13}\text{C}$  of c. 0.5‰ (Figs 4 and 5) during the Messinian may be partly explained by the global redistribution of carbon between land and ocean. In addition, continental shelf exposure owing to regressions during glacial conditions increased the local supply of refractory terrestrial organic matter with depleted  $\delta^{13}\text{C}$  from the exposed shelf areas. This effect has also been recorded in late Miocene sediments from the tropical Indian Ocean and Mediterranean Sea (Vincent *et al.* 1980; Loutit & Keigwin 1982; Kouwenhoven *et al.* 1999). Alternatively, drops in benthic  $\delta^{13}\text{C}$  values in the upper-slope

deposits of the Montemayor-1 core may be related either to the lateral entrainment of an ‘aged’ water mass or to the release of light  $^{12}\text{C}$  through remineralization of organic matter at times of enhanced upwelling with related high productivity and organic matter fluxes. The measured *C. pachydermus* prefers a very shallow infaunal microhabitat (Schmiedl *et al.* 2000) and may therefore incorporate a pore water signal.

Benthic foraminiferal assemblages assist discrimination between the possible processes controlling drops in benthic  $\delta^{13}\text{C}$  values. Upper-slope deposits of the Montemayor-1 core are characterized by high abundance of *Uvigerina peregrina s.l.* (Pérez-Asensio *et al.* 2012b; Fig. 4). This shallow-infaunal opportunistic species is characteristic of mesotrophic conditions (e.g. Schmiedl *et al.* 2000; Phipps *et al.* 2012) and preferentially inhabits upwelling areas with high supply of fresh marine organic matter as a food source (Fontanier *et al.* 2003; Koho *et al.* 2008; Schmiedl *et al.* 2010). Thus, elevated productivity associated with *Uvigerina peregrina s.l.* in the study area is most probably attributable to intensified upwelling related to AUW (Figs 2 and 6a). This interpretation is supported by a negative correlation between the abundance of *U. peregrina s.l.* and benthic  $\delta^{13}\text{C}$  values (Table 1).

These high-productivity conditions related to upwelling occurred during glacial periods (Fig. 6a), as indicated by the weak positive correlation between abundance of *U. peregrina s.l.* and benthic  $\delta^{18}\text{O}$  values (Table 1). This is also supported by observations from analogous modern environments (Schmiedl *et al.* 1997; Mendes *et al.* 2004; Martins *et al.* 2006; Mojtahid *et al.* 2006). The glacial enhancement of upwelling in the lower Guadalquivir Basin was probably caused by stronger winds promoting Ekman pumping similar to glacial intervals of the Quaternary (Lebreiro *et al.* 1997; Schmiedl & Mackensen 1997; Poli *et al.* 2010; Salgueiro *et al.* 2010). Model experiments on Messinian wind intensity and direction (Murphy *et al.* 2009) reveal intensified northwesterly winds that might have promoted upwelling conditions, similar to the present situation (Lebreiro *et al.* 1997). The remineralization of upwelling-related organic matter resulted in temporary oxygen depletions in the upper-slope settings during glacial periods (Fig. 5).

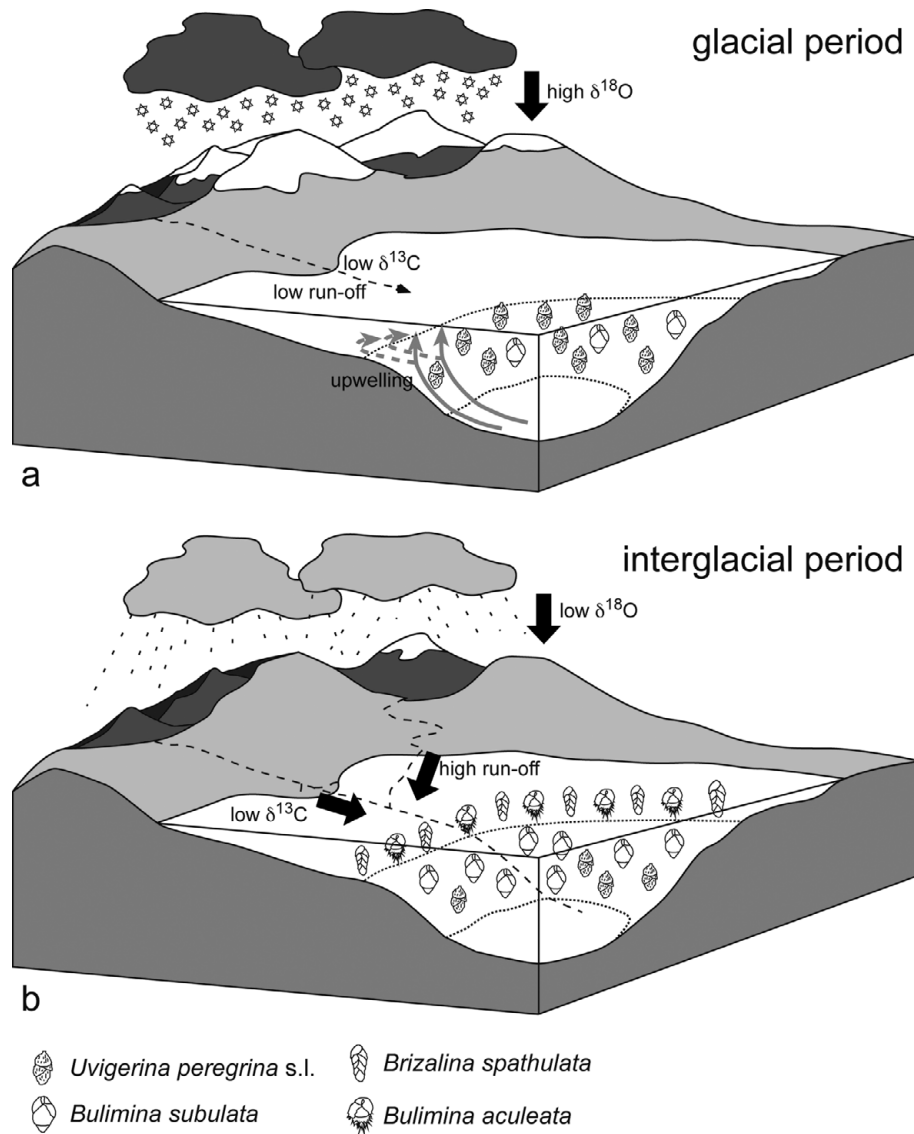


**Fig. 6.** Simplified conceptual models showing the interrelation between the various environmental factors (global palaeoclimate, river runoff and upwelling) that control palaeoproductivity and benthic foraminiferal distribution in the study case. (a) During glacial periods, both planktic and benthic oxygen isotopes show high values, whereas carbon isotopes show low values. Fresh organic matter comes from nutrient-enriched upwelling currents reaching the upper-middle-slope area. Benthic foraminiferal assemblages in the upper-middle slope are dominated by *Uvigerina peregrina s.l.* but *Bulimina subulata* is rare. (b) During interglacial periods,  $\delta^{18}\text{O}$  is low and  $\delta^{13}\text{C}$  is low. Intense rainfall increased runoff, thus degraded organic matter entered the ocean, favouring the profuse development of *Brizalina spathulata* and *Bulimina aculeata* in the outer shelf and *Bulimina subulata* in the upper-middle slope.

The abundance of *U. peregrina s.l.* is negatively correlated with the  $\delta^{13}\text{C}$  signal of the planktic *G. bulloides* (Table 1), which inhabits waters from surface to intermediate depths (20–300 m) (Pujol & Vergnaud-Grazzini 1995). Low  $\delta^{13}\text{C}$  values of *G. bulloides* are consistent with the upwelling of nutrient-rich,  $^{13}\text{C}$ -depleted intermediate waters. In addition, the  $\delta^{13}\text{C}$  signal of *G. bulloides* may have been influenced by variable vital effects (Lebreiro *et al.* 1997; Naidu & Niitsuma 2004).

Studies on modern planktonic foraminifera have shown that high nutrient availability is accompanied by faster calcification rates during strong upwelling events. This process is accompanied by higher respiration rates leading to the incorporation of more respired  $\text{CO}_2$ , enriched in  $^{12}\text{C}$ , into the test calcite (Naidu & Niitsuma 2004). Additionally, release of  $^{12}\text{C}$  during decomposition of organic matter in the lower part of the photic layer could contribute to the low  $\delta^{13}\text{C}$  observed in *G. bulloides*. These combined effects would explain the very low planktic  $\delta^{13}\text{C}$  signatures through the Montemayor-1 core.

In the upper-slope deposits of the Montemayor-1 core, peaks of *U. peregrina s.l.* alternate with high percentages of *Bulimina subulata* (Fig. 4). The former species, as mentioned above, dominated

during glacial periods and the latter during interglacial intervals (Figs 4 and 5). *Bulimina subulata*, like related species of the same genus, feeds on more degraded organic matter (Schmiedl *et al.* 2000; Diz & Francés 2008). The specific trophic preferences of the two dominant taxa might have accounted for the low abundances of *B. subulata* during glacial periods when fresh organic matter was available on the sea floor and the opportunistic *U. peregrina s.l.* dominated the foraminiferal assemblages. In contrast, *B. subulata* was abundant during interglacial periods, suggesting the presence of more degraded marine organic matter (Fig. 6b).

*Uvigerina peregrina s.l.* and *B. subulata* abundances decrease differently after 5.87 Ma (Fig. 4). At this point, *U. peregrina s.l.* disappears almost instantaneously whereas *B. subulata* diminishes gradually. Pérez-Asensio *et al.* (2012b) showed that the sharp reduction of *U. peregrina s.l.* coincided with an increase in epifaunal taxa, mainly *Planulina ariminensis*. This species inhabits oligotrophic shelf-edge settings, and thus the microfaunal replacement can be interpreted as a palaeoenvironmental shift from upper-slope to shelf-edge conditions (Pérez-Asensio *et al.* 2012b). The relatively high planktic  $\delta^{13}\text{C}$  values at the shelf edge suggest the absence of nutrient-rich upwelling waters in this setting (Fig. 4).

385  
386  
387  
388  
389  
390  
391  
392  
393  
394  
395  
396  
397  
398  
399  
400  
401  
402  
403  
404  
405  
406  
407  
408  
409  
410  
411  
412  
413  
414  
415  
416  
417  
418  
419  
420  
421  
422  
423  
424  
425  
426  
427  
428  
429  
430  
431  
432  
433  
434  
435  
436  
437  
438  
439  
440  
441  
442  
443  
444  
445  
446  
447  
448



The establishment of these particularly oligotrophic conditions on the shelf edge during a glacial period may have been caused by the presence of contour currents flowing along the platform margin that prevented the upwelling of intermediate waters (Fig. 2). As a consequence, the lack of sufficient fresh organic matter resulted in the sharp decrease in *U. peregrina s.l.* (Fig. 2). At the same time, *B. subulata* diminished more gradually than *U. peregrina s.l.* because more degraded organic matter was still present at the sea floor.

#### Outer platform degraded organic matter linked to continental runoff

The transition from a shelf edge to an outer shelf at 5.77 Ma, characterized by the disappearance of *Planulina ariminensis* (Pérez-Asensio *et al.* 2012b; Fig. 2), was coeval with a significant sea-level fall close to glacial stage TG 20 (5.75 Ma) (Pérez-Asensio *et al.* 2012a, 2012b, 2013; Jiménez-Moreno *et al.* 2013). From 5.77 to 5.67 Ma, the average values of planktic  $\delta^{13}\text{C}$  increased by 1‰ whereas average benthic  $\delta^{18}\text{O}$  values decreased by 0.9‰ (Fig. 4), pointing to a decrease in productivity most probably related to reduced influence of upwelling currents during interglacial conditions.

The outer-shelf deposits were characterized by high abundance of *Brizalina spathulata* and *Bulimina aculeata* (Pérez-Asensio *et al.* 2012b) (Fig. 4). Both species tolerate low-oxygen conditions and prefer environments with supply of continental degraded organic matter related to riverine discharges (Fig. 6b; Schmiedl *et al.* 2000, 2010; Donnici & Serandrei-Barbero 2002; Duchemin *et al.* 2008; Pérez-Asensio & Aguirre 2010), although *B. aculeata* is also able to feed on fresh organic matter (Schmiedl & Leuschner 2005). Therefore, the predominance of both *B. spathulata* and *B. aculeata* in our study can be taken to indicate supply of continental degraded organic matter related to riverine discharges (Fig. 6b).

The highest percentages of *Bulimina aculeata* and *Brizalina spathulata* on the outer shelf occurred during interglacial periods (Figs 4 and 6b) and alternated with peak abundances of the upwelling-related *U. peregrina s.l.* during glacial periods (Fig. 4). This inverse relationship, shown by a negative correlation between *U. peregrina s.l.* and *B. spathulata* (Table 1), points to renewed supply of fresh organic matter to the outer shelf from centres of upwelling during cool periods (Fig. 4).

In a global warming context, rainfall would have been high in many areas owing to the enhancement of the hydrological cycle (Frei *et al.* 1998). Palynological analysis in the Montemayor-1 core indicates that interglacial periods were characterized by warm and humid climates that promoted higher river runoff (Jiménez-Moreno *et al.* 2013; Fig. 6b). This is consistent with the gradual increase of *B. spathulata* concomitant with a long-term decrease of 0.7‰ in benthic  $\delta^{13}\text{C}$  values and 1.4‰ in planktic  $\delta^{13}\text{C}$  values, as well as low  $\delta^{18}\text{O}$  values from 5.67 to 5.38 Ma (Fig. 4). The shallowing upward trend in the core also supports the progressively larger influence of degraded organic matter in the outer-shelf deposits (Pérez-Asensio *et al.* 2012b). Repeated pulses of oxygen depletion on the outer shelf during interglacial periods can be associated with phases of particularly strong river runoff and input of terrestrial organic matter (Fig. 5).

Strongly depleted  $\delta^{13}\text{C}$  values of *G. bulloides* at 5.44 and 5.41 Ma (Figs 4 and 5) may reflect enhanced rainfall, as recorded in sediments from the Mallorca shelf during the early Holocene humid phase (Milker *et al.* 2012). Increased humidity could have been related to global warming linked to interglacial stage TG 11 (5.52 Ma), which commenced before the Miocene–Pliocene boundary and persisted until the mid-Pliocene (Vidal *et al.* 2002; Jiménez-Moreno *et al.* 2013; Pérez-Asensio *et al.* 2013).

#### Effect of the Mediterranean Outflow Water interruption on palaeoproductivity in the northeastern Atlantic during the Messinian

Our results document temporal variations in productivity and carbon cycling in the northeastern Atlantic Ocean during the Messinian. This was an important time period that led to one of the most dramatic episodes in the geologically recent history of the Mediterranean Sea. Progressive restriction of the various Betic and Rifian corridors connecting the Atlantic and Mediterranean resulted in the isolation of the Mediterranean from the world ocean (Benson *et al.* 1991; Martín & Braga 1994; Esteban *et al.* 1996; Riding *et al.* 1998; Krijgsman *et al.* 1999; Martín *et al.* 2001; Braga *et al.* 2006). This, in turn, forced the formation of extensive evaporite deposits in the central Mediterranean and in its peripheral basins during the Messinian ‘Salinity Crisis’ (Hsü *et al.* 1973, 1977).

The Montemayor-1 core is located close to the last active Betic gateway, the Guadalhorce Corridor, which closed at 6.18 Ma (Martín *et al.* 2001; Pérez-Asensio *et al.* 2012a, 2013). The final closure of the corridors terminated Mediterranean–Atlantic water exchange through the Betic straits. This in turn altered the circulation patterns in the NE Atlantic (Pérez-Asensio *et al.* 2012a), affecting the regional surface water productivity. In this section, we analyse how the interplay of the Mediterranean Outflow Water and NE Atlantic palaeocurrents affected primary production before and after closure of the Guadalhorce Corridor. This issue has been largely overlooked by researchers (but see van der Laan *et al.* 2006, 2012) and is crucial to understanding of the ultimate consequences of Mediterranean isolation.

Low abundance of *U. peregrina s.l.* and high benthic  $\delta^{13}\text{C}$  values at 6.44 and 6.24 Ma (Fig. 4) indicate the presence of well-ventilated bottom waters with low organic fluxes to the sea floor. This probably implies the presence of MOW that was characterized by a high  $\delta^{13}\text{C}$  signature relative to Atlantic waters, reflecting the relatively low residence time of the MOW (Vergnaud-Grazzini 1983; Schönfeld & Zahn 2000; Raddatz *et al.* 2011). Presence of the MOW would have increased bottom-water oxygenation, as shown by the relatively high oxygen content prior to interruption of this current at 6.18 Ma (Figs 5 and 7a) when the Guadalhorce Corridor was finally closed (Pérez-Asensio *et al.* 2012a). High benthic  $\delta^{13}\text{C}$  values during interglacial periods may also be related to well-ventilated bottom waters linked to a strong Atlantic meridional overturning circulation (AMOC), as occurred during the Quaternary (Broecker *et al.* 1985).

In contrast, high abundance of *U. peregrina s.l.* and coinciding low benthic  $\delta^{13}\text{C}$  values at 6.67 and 6.35 Ma (Fig. 4) point to the influence of low-oxygen AYW (Fig. 7b). In addition, low benthic  $\delta^{13}\text{C}$  values in Atlantic and Caribbean Messinian records suggest a general reduction of the AMOC, provoked by low North Atlantic Deep Water formation during glacial conditions (Zahn *et al.* 1997; Bickert *et al.* 2004; van der Laan *et al.* 2012; Fig. 7b).

After closure of the Guadalhorce Corridor at 6.18 Ma, there was a gradual decrease of 0.8‰ in benthic  $\delta^{13}\text{C}$  values that can be related to the interruption of the MOW and the influence of nutrient and  $^{12}\text{C}$ -rich AYW (Figs 4 and 7c). The planktic  $\delta^{13}\text{C}$  values show a progressive decrease of 1.3‰, also indicating the AYW influence. Concomitantly, *U. peregrina s.l.*, which thrives under upwelling conditions, gradually increased to its highest abundance (Fig. 4). Therefore, after cessation of the MOW, only AYW reached the upper slope in the study area, promoting high productivity (Fig. 7c). In addition, high productivity could have been favoured by cessation of the MOW, which weakened the AMOC and promoted northern hemisphere cooling, as shown by the onset of some increase in ice sheets in the Iceland–Norwegian Sea and Baffin Bay

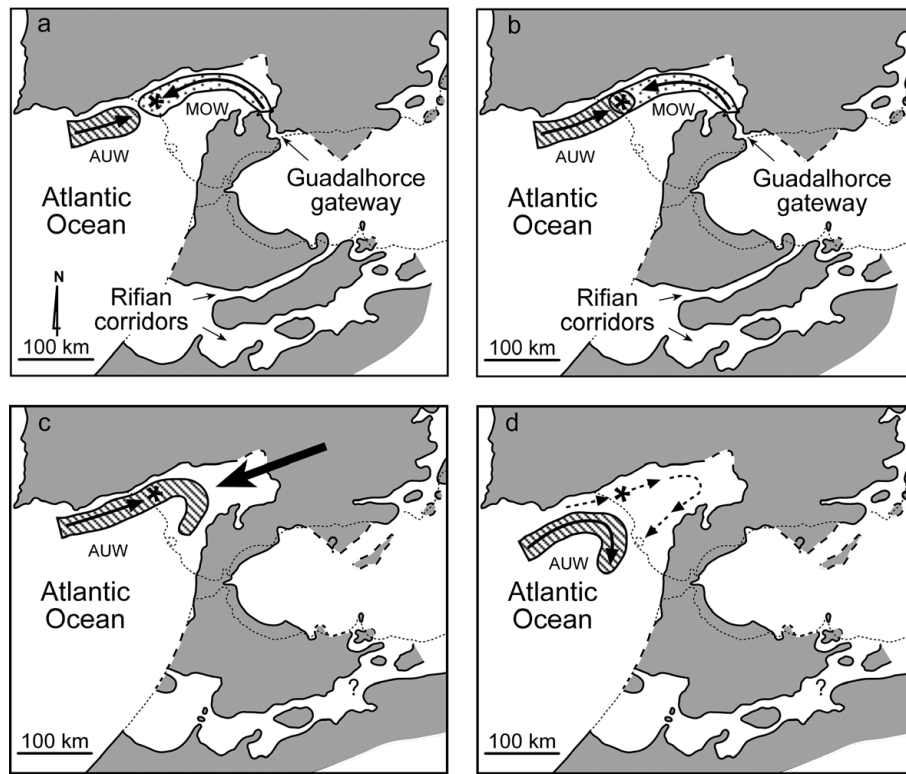


**Fig. 7.** Palaeogeographical and palaeoceanographical evolution of the lower Guadalquivir Basin during the Messinian (based on Martín *et al.* (2009)). (a) Interglacial conditions before 6.18 Ma, when only the Mediterranean Outflow Water (MOW) reached the location of the studied core (asterisk). (b) Glacial conditions before 6.18 Ma, when both Atlantic Upwelled Water (AUW) and the MOW reached the study site. (c) Glacial conditions after 6.18 Ma, when only AUW reached the site because the MOW was interrupted. The wide black arrow marks the progradation of the main depositional systems along the axis of the Guadalquivir Basin. (d) The study location (asterisk) was influenced by currents along the shelf-break (dashed arrows) that prevented the AUW from reaching the study area between 5.87 and 5.77 Ma.

(Alaska) at *c.* 7–6 Ma (Fronval & Jansen 1996; Thiede *et al.* 1998; Pérez-Asensio *et al.* 2012a). This cooling would have intensified trade winds that enhanced upwelling (Hughen *et al.* 1996; Clark *et al.* 2002).

During the transition from middle–upper-slope to shelf-edge deposits between 5.87 and 5.77 Ma (Figs 2 and 4), well after corridor closing, oligotrophic conditions prevailed as mentioned above. The local reduction of productivity was probably related to currents parallel to the shelf-break that prevented the AUW from reaching the study area (Fig. 7d).

## Conclusions

Palaeoproductivity changes and organic carbon cycling in the northeastern Atlantic during the Messinian were intimately connected with global glacioeustasy. Glacial periods (cold and dry climate) were characterized by high planktic and benthic  $\delta^{18}\text{O}$  values, low benthic  $\delta^{13}\text{C}$  values, high abundance of *U. peregrina s.l.*, and moderate oxygen depletion. These results point to high productivity related to upwelling currents during glacial periods. The upwelling was produced by Ekman pumping owing to intensified northwesterly trade winds. In contrast, interglacial periods (warm and humid climate) show low planktic and benthic  $\delta^{18}\text{O}$  values, high oxygen depletion and high abundance of *B. subulata* in the upper slope, and of *B. spathulata* and *B. aculeata* in the outer shelf. These results suggest the presence of more degraded marine organic matter in the upper slope and a supply of degraded continental organic matter derived from enhanced river runoff and transport to the outer shelf.

Before closure of the Guadalquivir Corridor, which was the final Betic Atlantic–Mediterranean gateway, the study area was alternately influenced by the well-ventilated MOW and poorly ventilated AUW. Once this Betic seaway was closed at 6.18 Ma, the interruption of the MOW reduced the AMOC and promoted glacial

conditions in the northern hemisphere, thus favouring high-productivity conditions in the study region. Our data show how cessation of the MOW caused global oceanographic and climatic changes that affected productivity in the northern hemisphere. In addition, variability in the AMOC is recorded by fluctuations in benthic  $\delta^{13}\text{C}$  values. High benthic  $\delta^{13}\text{C}$  values indicate well-ventilated bottom waters owing to strong AMOC during interglacial periods. In contrast, low values reflect poor ventilation as a result of weak AMOC during glacial periods.

We are very grateful to two anonymous reviewers and the editor J. Hendry for their thorough reviews of an early version of the paper. This work was funded by the Research Projects CGL2010-20857 and CGL2009-11539/BTE of the Ministerio de Ciencia e Innovación of Spain, and the Research Group RNM-190 of the Junta de Andalucía. J.N.P.A. was funded by a research F.P.U. grant (ref. AP2007-00345) awarded by the Ministerio de Educación of Spain. We thank N. Andersen (Leibniz-Laboratory, Kiel, Germany) for stable isotope analyses, R. Riding for checking the English text, and E. Samankassou for reading the paper and his suggestions.

## References

- AGUIRRE, J. 1992. Evolución de las asociaciones fósiles del Plioceno marino de Cabo Roche (Cádiz). *Revista Española de Paleontología Extra*, **3**, 3–10.
- AGUIRRE, J. 1995. Implicaciones paleoambientales y paleogeográficas de dos discontinuidades estratigráficas en los depósitos pliocénicos de Cádiz (SW de España). *Revista de la Sociedad Geológica de España*, **8**, 161–174.
- AGUIRRE, J., CASTILLO, C., FÉRRIZ, F.J., AGUSTÍ, J. & OMS, O. 1995. Marine–continental magnetobiostratigraphic correlation of the *Dolomys* subzone (middle of Late Ruscinian): Implications for the Late Ruscinian age. *Palaeogeography, Palaeoclimatology, Palaeoecology*, **117**, 139–152. [http://dx.doi.org/10.1016/0031-0182\(94\)00123-P](http://dx.doi.org/10.1016/0031-0182(94)00123-P).
- AGUIRRE, J., BRAGA, J.C. & MARTÍN, J.M. 2007. El Mioceno marino del Prebético occidental (Cordillera Bética, SE de España): historia del cierre del Estrecho Norbético. In: AGUIRRE, J., COMPANY, M. & RODRÍGUEZ-TOVAR, F.J. (eds) *XIII Jornadas de la Sociedad Española de Paleontología: Guía de Excursiones*. Instituto Geológico y Minero de España, Madrid; Universidad de Granada, Granada, 53–66.

513  
514  
515  
516  
517  
518  
519  
520  
521  
522  
523  
524  
525  
526  
527  
528  
529  
530  
531  
532  
533  
534  
535  
536  
537  
538  
539  
540  
541  
542  
543  
544  
545  
546  
547  
548  
549  
550  
551  
552  
553  
554  
555  
556  
557  
558  
559  
560  
561  
562  
563  
564  
565  
566  
567  
568  
569  
570  
571  
572  
573  
574  
575  
576

- 577 ANFUSO, E., DEBELIUS, B., CASTRO, C.G., PONCE, R., FORJA, J.M. & LUBIAN,  
578 L.M. 2013. Seasonal evolution of chlorophyll-a and cyanobacteria  
579 (*Prochlorococcus* and *Synechococcus*) on the northeast continental shelf of  
580 the Gulf of Cádiz: Relation to thermohaline and nutrients fields. *Scientia*  
581 *Marina*, **77**, 25–36, <http://dx.doi.org/10.3989/scimar.03730.27A>.
- 582 BACETA, J.I. & PENDÓN, J.G. 1999. Estratigrafía y arquitectura de facies de la  
583 Formación Niebla, Neógeno superior, sector occidental de la Cuenca del  
584 Guadalquivir. *Revista de la Sociedad Geológica de España*, **12**, 419–438.
- 585 BAKUN, A., FIELD, D.B., REDONDO-RODRIGUEZ, A. & WEEKS, S.J. 2010.  
586 Greenhouse gas, upwelling-favorable winds, and the future of coastal ocean  
587 upwelling ecosystems. *Global Change Biology*, **16**, 1213–1228, <http://dx.doi.org/10.1111/j.1365-2486.2009.02094.x>.
- 588 BENSON, R.H., RAKIC-EL BIED, K. & BONADUCE, G. 1991. An important current  
589 reversal (influx) in the Rifian corridor (Morocco) at the Tortonian–  
590 Messinian Boundary: The end of Tethys ocean. *Paleoceanography*, **6**,  
591 164–192, <http://dx.doi.org/10.1029/90PA00756>.
- 592 BETZLER, C., BRAGA, J.C., MARTÍN, J.M., SÁNCHEZ-ALMAZO, I.M. & LINDHORST, S.  
593 2006. Closure of a seaway: Stratigraphic record and facies (Guadix basin,  
594 southern Spain). *International Journal of Earth Sciences*, **95**, 903–910,  
595 <http://dx.doi.org/10.1007/s00531-006-0073-y>.
- 596 BICKERT, T., HAUG, G.H. & TIEDEMANN, R. 2004. Late Neogene benthic stable isotope  
597 record of Ocean Drilling Program Site 999: Implications for Caribbean  
598 paleoceanography, organic carbon burial, and the Messinian Salinity Crisis.  
599 *Paleoceanography*, **19**, <http://dx.doi.org/10.1029/2002PA000799>.
- 600 BRAGA, J.C., MARTÍN, J.M. & AGUIRRE, J. 2002. Tertiary. Southern Spain. In:  
601 GIBBONS, W. & MORENO, T. (eds) *The Geology of Spain*. Geological Society,  
602 London, 320–327.
- 603 BRAGA, J.C., MARTÍN, J.M. & QUESADA, C. 2003. Patterns and average rates of late  
604 Neogene–Recent uplift of the Betic Cordillera, SE Spain. *Geomorphology*,  
605 **50**, 3–26, [http://dx.doi.org/10.1016/S0169-555X\(02\)00205-2](http://dx.doi.org/10.1016/S0169-555X(02)00205-2).
- 606 BRAGA, J.C., MARTÍN, J.M., RIDING, R., AGUIRRE, J., SÁNCHEZ-ALMAZO, I.M. &  
607 DINARÉS-TURELL, J. 2006. Testing models for the Messinian salinity crisis:  
608 The Messinian record in Almería, SE Spain. *Sedimentary Geology*, **188–**  
609 **189**, 131–154, <http://dx.doi.org/10.1016/j.sedgeo.2006.03.002>.
- 610 BRAGA, J.C., VESCOGNI, A., BOSELLINI, F.R. & AGUIRRE, J. 2009. Coralline algae  
611 (Corallinales, Rhodophyta) in western and central Mediterranean Messinian  
612 reefs. *Palaeogeography, Palaeoclimatology, Palaeoecology*, **275**, 113–128,  
613 <http://dx.doi.org/10.1016/j.palaeo.2009.02.022>.
- 614 BRAGA, J.C., MARTÍN, J.M., ET AL. 2010. Middle-Miocene (Serravallian) temperate  
615 carbonates in a seaway connecting the Atlantic Ocean and the  
616 Mediterranean Sea (North Betic Strait, S Spain). *Sedimentary Geology*, **225**,  
617 19–33, <http://dx.doi.org/10.1016/j.sedgeo.2010.01.003>.
- 618 BROECKER, W.S., PETEET, D.M. & RIND, D. 1985. Does the ocean–atmosphere  
619 system have more than one stable mode of operation? *Nature*, **315**, 21–26,  
620 <http://dx.doi.org/10.1038/315021a0>.
- 621 CABEÇADAS, G. & BROGUEIRA, M.J. 1997. Sediments in a Portuguese coastal area—  
622 pool sizes of mobile and immobile forms of nitrogen and phosphorus.  
623 *Marine and Freshwater Research*, **48**, 559–563, <http://dx.doi.org/10.1071/MF96053>.
- 624 CIVIS, J., SIERRO, F.J., GONZÁLEZ-DELGADO, J.A., FLORES, J.A., ANDRÉS, I., DE  
625 PORTA, J. & VALLE, M.F. 1987. El Neógeno marino de la provincia de  
626 Huelva: Antecedentes y definición de las unidades litoestratigráficas. In:  
627 CIVIS, J. (ed.) *Paleontología del Neógeno de Huelva*. Ediciones Universidad  
628 de Salamanca, Salamanca, 9–21.
- 629 CLARK, P.U., PISIAS, N.G., STOCKER, T.F. & WEAVER, A.J. 2002. The role of the  
630 thermohaline circulation in abrupt climate change. *Nature*, **415**, 863–869,  
631 <http://dx.doi.org/10.1038/415863a>.
- 632 DIZ, P. & FRANCÉS, G. 2008. Distribution of live benthic foraminifera in the  
633 Ría de Vigo (NW Spain). *Marine Micropaleontology*, **66**, 165–191, <http://dx.doi.org/10.1016/j.marmicro.2007.09.001>.
- 634 DONNICI, S. & SERANDREI-BARBERO, R. 2002. The benthic foraminiferal commu-  
635 nities of the northern Adriatic continental shelf. *Marine Micropaleontology*,  
636 **44**, 93–123, [http://dx.doi.org/10.1016/S0377-8398\(01\)00043-3](http://dx.doi.org/10.1016/S0377-8398(01)00043-3).
- 637 DUCHEMIN, G., JORISSEN, F.J., LELOC'H, F., ANDRIEUX-LOYER, F., HILY, C. &  
638 THOUZEAU, G. 2008. Seasonal variability of living benthic foraminifera from  
639 the outer continental shelf of the Bay of Biscay. *Journal of Sea Research*,  
640 **59**, 297–319, <http://dx.doi.org/10.1016/j.seares.2008.03.006>.
- 641 EBERWEIN, A. & MACKENSEN, A. 2006. Live and dead benthic foraminifera  
642 and test  $\delta^{13}\text{C}$  record primary productivity off Morocco (NW Africa).  
643 *Deep-Sea Research, Part I*, **53**, 1379–1405, <http://dx.doi.org/10.1016/j.dsr.2006.04.001>.
- 644 EBERWEIN, A. & MACKENSEN, A. 2008. Last Glacial Maximum paleoproductivity  
645 and water masses off NW Africa: Evidence from benthic foraminifera  
646 and stable isotopes. *Marine Micropaleontology*, **67**, 87–103, <http://dx.doi.org/10.1016/j.marmicro.2007.08.008>.
- 647 ESTEBAN, M., BRAGA, J.C., MARTÍN, J.M. & SANTISTEBAN, C. 1996. Western  
648 Mediterranean reef complexes. In: FRANSEEN, E.K., ESTEBAN, M., WARD,  
649 W.C. & ROUCHY, J.M. (eds) *Models for Carbonate Stratigraphy from*  
650 *Miocene Reef Complexes of Mediterranean Regions*. Society of Economic  
651 Paleontologists and Mineralogists, Concepts in Sedimentology and  
652 Paleontology, **5**, 55–72.
- 653 FONTANIER, C., JORISSEN, F.J., CHAILLOU, G., DAVID, C., ANSCHUTZ, P. & LAFON, V.  
654 2003. Seasonal and interannual variability of benthic foraminiferal faunas at  
655 550 m depth in the Bay of Biscay. *Deep-Sea Research, Part I*, **50**, 457–494,  
656 [http://dx.doi.org/10.1016/S0967-0637\(02\)00167-X](http://dx.doi.org/10.1016/S0967-0637(02)00167-X).
- 657 FREI, C., SCHÄR, C., LÜTHI, D. & DAVIES, H.C. 1998. Heavy precipitation pro-  
658 cesses in warmer climate. *Geophysical Research Letters*, **25**, 1431–1434,  
659 <http://dx.doi.org/10.1029/98GL51099>.
- 660 FRONVAL, T. & JANSEN, E. 1996. Late Neogene paleoclimates and paleocean-  
661 ography in the Iceland–Norwegian Sea: Evidence from the Iceland and  
662 Vøring Plateaus. In: MYHRE, A.M., THIEDE, J., ET AL. (eds) Proceedings of  
663 the Ocean Drilling Program, Scientific Results, **151**, 455–468, <http://dx.doi.org/10.2973/odp.proc.sr.151.134.1996>.
- 664 GOINEAU, A., FONTANIER, C., ET AL. 2011. Live (stained) benthic foraminifera from  
665 the Rhône prodelta (Gulf of Lion, NW Mediterranean): Environmental con-  
666 trols on a river-dominated shelf. *Journal of Sea Research*, **65**, 58–75, <http://dx.doi.org/10.1016/j.seares.2010.07.007>.
- 667 HAMMER, Ø., HARPER, D.A.T. & RYAN, P.D. 2001. PAST: Paleontological  
668 Statistics software package for education and data analysis. *Palaeontologia*  
669 *Electronica*, **4**, 1–9.
- 670 HSÜ, K.J., RYAN, W.B.F. & CITA, M.B. 1973. Late Miocene desiccation of the  
671 Mediterranean. *Nature*, **242**, 240–244, <http://dx.doi.org/10.1038/242240a0>.
- 672 HSÜ, J.K., MONTADERT, L., ET AL. 1977. History of the Mediterranean salinity  
673 crisis. *Nature*, **267**, 1053–1078, <http://dx.doi.org/10.1038/267399a0>.
- 674 HUGHEN, K.A., OVERPECK, J.T., PETERSON, L.C. & TRUMBORE, S. 1996. Rapid climate  
675 changes in the tropical Atlantic region during the last deglaciation.  
676 *Nature*, **380**, 51–54, <http://dx.doi.org/10.1038/380051a0>.
- 677 JIMÉNEZ-MORENO, G., PÉREZ-ASENSIO, J.N., ET AL. 2013. Vegetation, sea-level and  
678 climate changes during the Messinian salinity crisis. *Geological Society of*  
679 *America Bulletin*, **125**, 432–444, <http://dx.doi.org/10.1130/B30663.1>.
- 680 JORISSEN, F.J., BARMAWIDJAJA, D.M., PUSKARIC, S. & VAN DER ZWAAN, G.J. 1992.  
681 Vertical distribution of benthic foraminifera in the northern Adriatic Sea:  
682 The relation with the organic flux. *Marine Micropaleontology*, **19**, 131–146,  
683 [http://dx.doi.org/10.1016/0377-8398\(92\)90025-F](http://dx.doi.org/10.1016/0377-8398(92)90025-F).
- 684 JORISSEN, F.J., DE STIGTER, H.C. & WIDMARK, J.G.V. 1995. A conceptual model  
685 explaining benthic foraminiferal microhabitats. *Marine Micropaleontology*,  
686 **26**, 3–15.
- 687 KOHO, K.A., GARCÍA, R., DE STIGTER, H.C., EPPING, E., KONING, E., KOUWENHOVEN,  
688 T.J. & VAN DER ZWAAN, G.J. 2008. Sedimentary labile organic carbon and  
689 pore water redox control on species distribution of benthic foraminifera: A  
690 case study from Lisbon–Setúbal Canyon (southern Portugal). *Progress in*  
691 *Oceanography*, **79**, 55–82, <http://dx.doi.org/10.1016/j.poccean.2008.07.004>.
- 692 KOUWENHOVEN, T.J., SEIDENKRANTZ, M.-S. & VAN DER ZWAAN, G.J. 1999. Deep-  
693 water changes: the near-synchronous disappearance of a group of benthic  
694 foraminifera from the Late Miocene Mediterranean. *Palaeogeography,*  
695 *Palaeoclimatology, Palaeoecology*, **152**, 259–281, [http://dx.doi.org/10.1016/S0031-0182\(99\)00065-6](http://dx.doi.org/10.1016/S0031-0182(99)00065-6).
- 696 KRUGSMAN, W., HILGEN, F.J., RAFFI, I., SIERRO, F.J. & WILSON, D.S. 1999.  
697 Chronology, causes and progression of the Messinian salinity crisis. *Nature*,  
698 **400**, 652–655, <http://dx.doi.org/10.1038/23231>.
- 699 LARRASOÑA, J.C., GONZÁLEZ-DELGADO, J.A., CIVIS, J., SIERRO, F.J., ALONSO-  
700 GAVILÁN, G. & PAIS, J. 2008. Magnetobiostratigraphic dating and envi-  
701 ronmental magnetism of Late Neogene marine sediments recovered at the  
702 Huelva-1 and Montemayor-1 boreholes (lower Guadalquivir basin, Spain).  
703 *Geo-Temas*, **10**, 1175–1178.
- 704 LEBREIRO, S.M., MORENO, J.C., ABRANTES, F.F. & PFLAUMANN, U. 1997.  
705 Productivity and paleoceanographic implications on the Tore Seamount  
706 (Iberian Margin) during the last 225 kyr: foraminiferal evidence.  
707 *Paleoceanography*, **12**, 718–727, <http://dx.doi.org/10.1029/97PA01748>.
- 708 LEBREIRO, S.M., FRANCÉS, G., ET AL. 2006. Climate change and coastal hydro-  
709 graphic response along the Atlantic Iberian margin (Tagus Prodelt and  
710 Muros Ria) during the last two millennia. *Holocene*, **16**, 1003–1015, <http://dx.doi.org/10.1177/0959683606h1990rp>.
- 711 LOURENS, L.J., HILGEN, F.J., SHACKLETON, N.J., LASKAR, J. & WILSON, D.S. 2004.  
712 The Neogene Period. In: GRADSTEIN, F.M., OGG, J.G. & SMITH, A.G. (eds)  
713 *A Geologic Time Scale 2004*. Cambridge University Press, Cambridge,  
714 409–440.
- 715 LOUITT, T.S. & KEIGWIN, L.D. 1982. Stable isotopic evidence for latest Miocene  
716 sea-level fall in the Mediterranean region. *Nature*, **300**, 163–166, <http://dx.doi.org/10.1038/300163a0>.
- 717 LYLE, M.W., PRAHL, F.G. & SPARROW, M.A. 1992. Upwelling and productivity  
718 changes inferred from a temperature record in the central equatorial Pacific.  
719 *Nature*, **355**, 812–815, <http://dx.doi.org/10.1038/355812a0>.
- 720 MACKENSEN, A. 2008. On the use of benthic foraminiferal  $\delta^{13}\text{C}$  in paleocean-  
721 ography: constraints from primary proxy relationships. In: AUSTIN, W.E.N.  
722 & JAMES, R.H. (eds) *Biogeochemical Controls on Palaeoceanographic*  
723 *Environmental Proxies*. Geological Society, London, Special Publications,  
724 **303**, 121–133.

- MARTÍN, J.M. & BRAGA, J.C. 1994. Messinian events in the Sorbas basin in southeastern Spain and their implications in the recent history of the Mediterranean. *Sedimentary Geology*, **90**, 257–268, [http://dx.doi.org/10.1016/0037-0738\(94\)90042-6](http://dx.doi.org/10.1016/0037-0738(94)90042-6).
- MARTÍN, J.M., BRAGA, J.C. & BETZLER, C. 2001. The Messinian Guadalhorca Corridor: the last northern, Atlantic–Mediterranean gateway. *Terra Nova*, **13**, 418–424, <http://dx.doi.org/10.1046/j.1365-3121.2001.00376.x>.
- MARTÍN, J.M., BRAGA, J.C., AGUIRRE, J. & PUGA-BERNABEU, A. 2009. History and evolution of the North-Betic Strait (Prebetic Zone, Betic Cordillera): A narrow, early Tortonian, tidal-dominated, Atlantic–Mediterranean marine passage. *Sedimentary Geology*, **216**, 80–90, <http://dx.doi.org/10.1016/j.sedgeo.2009.01.005>.
- MARTINEZ, P., BERTRAND, B., SHIMMIEDL, G.B., COCHRANE, K., JORISSEN, J., FOSTER, J.M. & DIGNAN, M. 1999. Upwelling intensity and ocean productivity changes off Cape Blanc (Northwest Africa) during the last 70,000 years: Geochemical and micropaleontological evidence. *Marine Geology*, **158**, 57–74, [http://dx.doi.org/10.1016/S0025-3227\(98\)00161-3](http://dx.doi.org/10.1016/S0025-3227(98)00161-3).
- MARTINS, V., JOUANNEAU, J.-M., WEBER, O. & ROCHA, F. 2006. Tracing the late Holocene evolution of the NW Iberian upwelling system. *Marine Micropaleontology*, **59**, 35–55, <http://dx.doi.org/10.1016/j.marmicro.2005.12.002>.
- MAYORAL, E. & PENDÓN, J.G. 1987. Icnofacies y sedimentación en zona costera. Plioceno superior (?), litoral de Huelva. *Acta Geológica Hispánica*, **21–22**, 507–513.
- MCCORKLE, D.C., KEIGWIN, L.D., CORLISS, B.H. & EMERSON, S.R. 1990. The influence of microhabitats on the carbon isotopic composition of deep-sea benthic foraminifera. *Paleoceanography*, **5**, 161–185.
- MCKEE, B.A., ALLER, R.C., ALLISON, M.A., BIANCHI, T.S. & KINEKE, G.C. 2004. Transport and transformation of dissolved and particulate materials on continental margins influenced by major rivers: Benthic boundary layer and seabed processes. *Continental and Shelf Research*, **24**, 899–926, <http://dx.doi.org/10.1016/j.csr.2004.02.009>.
- MCMANUS, J.F., FRANCOIS, R., GHERARDI, J.M., KEIGWIN, L.D. & BROWN-LEGER, S. 2004. Collapse and rapid resumption of Atlantic meridional circulation linked to deglacial climate changes. *Nature*, **428**, 834–837, <http://dx.doi.org/10.1038/nature02494>.
- MENDES, I., GONZALEZ, R., DIAS, J.M.A., LOBO, F. & MARTINS, V. 2004. Factors influencing recent benthic foraminifera distribution on the Guadiana shelf (Southwestern Iberia). *Marine Micropaleontology*, **51**, 171–192, <http://dx.doi.org/10.1016/j.marmicro.2003.11.001>.
- MILKER, Y., SCHMIEDL, G., BETZLER, C., ANDERSEN, N. & THEODOR, M. 2012. Response of Mallorca shelf ecosystems to an early Holocene humid phase. *Marine Micropaleontology*, **90–91**, 1–12, <http://dx.doi.org/10.1016/j.marmicro.2012.04.001>.
- MOJTAHID, M., JORISSEN, F., DURRIEU, J., GALGANI, F., HOWA, H., REDOIS, F. & CAMPS, R. 2006. Benthic foraminifera as bio-indicators of drill cutting disposal in tropical east Atlantic outer shelf environments. *Marine Micropaleontology*, **61**, 58–75, <http://dx.doi.org/10.1016/j.marmicro.2006.05.004>.
- MURPHY, L.N., KIRK-DAVIDOFF, D.B., MAHOWALD, N. & OTTO-BLIESNER, B.L. 2009. A numerical study of the climate response to lowered Mediterranean Sea level during the Messinian Salinity Crisis. *Paleogeography, Palaeoclimatology, Palaeoecology*, **279**, 41–59, <http://dx.doi.org/10.1016/j.palaeo.2009.04.016>.
- MURRAY, J.W. 2006. *Ecology and Applications of Benthic Foraminifera*. Cambridge University Press, Cambridge.
- NAIDU, P. & NITSUMA, N. 2004. Atypical  $\delta^{13}\text{C}$  signature in *Globigerina bulloides* at the ODP Site 723An (Arabian Sea): Implications of environmental changes caused by upwelling. *Marine Micropaleontology*, **53**, 1–10, <http://dx.doi.org/10.1016/j.marmicro.2004.01.005>.
- PÉREZ-ASENSIO, J.N. & AGUIRRE, J. 2010. Benthic foraminiferal assemblages in temperate coral-bearing deposits from the Late Pliocene. *Journal of Foraminiferal Research*, **40**, 61–78, <http://dx.doi.org/10.2113/gsjfr.40.1.61>.
- PÉREZ-ASENSIO, J.N., AGUIRRE, J., SCHMIEDL, G. & CIVIS, J. 2012a. Impact of restriction of the Atlantic–Mediterranean gateway on the Mediterranean Outflow Water and eastern Atlantic circulation during the Messinian. *Paleoceanography*, **27**, PA3222, <http://dx.doi.org/10.1029/2012PA002309>.
- PÉREZ-ASENSIO, J.N., AGUIRRE, J., SCHMIEDL, G. & CIVIS, J. 2012b. Messinian paleoenvironmental evolution in the lower Guadalquivir Basin (SW Spain) based on benthic foraminifera. *Paleogeography, Palaeoclimatology, Palaeoecology*, **326–328**, 135–151, <http://dx.doi.org/10.1016/j.palaeo.2012.02.014>.
- PÉREZ-ASENSIO, J.N., AGUIRRE, J., JIMÉNEZ-MORENO, G., SCHMIEDL, G. & CIVIS, J. 2013. Glacioeustatic control on the origin and cessation of the Messinian salinity crisis. *Global and Planetary Change*, **111**, 1–8, <http://dx.doi.org/10.1016/j.gloplacha.2013.08.008>.
- PHIPPS, M., JORISSEN, F., PUSCEDDU, A., BIANCHELLI, S. & DE STIGTER, H. 2012. Live benthic foraminiferal faunas along a bathymetrical transect (282–4987 m) on the Portuguese margin (NE Atlantic). *Journal of Foraminiferal Research*, **42**, 66–81, <http://dx.doi.org/10.2113/gsjfr.42.1.66>.
- PIOTROWSKI, A.M., GOLDSTEIN, S.L., HEMMING, S.R. & FAIRBANKS, R.G. 2005. Temporal relationships of carbon cycling and ocean circulation at glacial boundaries. *Science*, **307**, 1933–1938, <http://dx.doi.org/10.1126/science.1104883>.
- POLI, M.S., MEYERS, P.A. & THUNELL, R.C. 2010. The western North Atlantic record of MIS 13 to 10: Changes in primary productivity, organic carbon accumulation and benthic foraminiferal assemblages in sediments from the Blake Outer Ridge (ODP Site 1058). *Paleogeography, Palaeoclimatology, Palaeoecology*, **295**, 89–101, <http://dx.doi.org/10.1016/j.palaeo.2010.05.018>.
- PUJOL, C. & VERGNAUD-GRAZZINI, C. 1995. Distribution patterns of live planktic foraminifera as related to regional hydrography and productive systems of the Mediterranean Sea. *Marine Micropaleontology*, **25**, 187–217, [http://dx.doi.org/10.1016/0377-8398\(95\)00002-1](http://dx.doi.org/10.1016/0377-8398(95)00002-1).
- RADDATZ, J., RÜGGERBERG, A., MARGRETH, S., DULLO, W.-C. & IODP EXPEDITION 307 SCIENTIFIC PARTY 2011. Paleoenvironmental reconstruction of Challenger Mound initiation in the Porcupine Seabight, NE Atlantic. *Marine Geology*, **282**, 79–90, <http://dx.doi.org/10.1016/j.margeo.2010.10.019>.
- RAHMSTORF, S. 1998. Influence of Mediterranean Outflow on climate. *EOS Transactions, American Geophysical Union*, **79**, 281–282, <http://dx.doi.org/10.1029/98EO00208>.
- RIAZA, C. & MARTÍNEZ DEL OLMO, W. 1996. Depositional model of the Guadalquivir–Gulf of Cádiz Tertiary basin. In: FRIEND, P. & DABRIO, C.J. (eds) *Tertiary Basins of Spain*. Cambridge University Press, Cambridge, 330–338.
- RIDING, R., BRAGA, J.C., MARTÍN, J.M. & SÁNCHEZ-ALMAZO, I.M. 1998. Mediterranean Messinian salinity crisis: Constraints from a coeval marginal basin, Sorbas, southeastern Spain. *Marine Geology*, **146**, 1–20, [http://dx.doi.org/10.1016/S0025-3227\(97\)00136-9](http://dx.doi.org/10.1016/S0025-3227(97)00136-9).
- RODRIGUES, T., GRIMALT, J.O., ABRANTES, F., FLORES, J.A. & LEBREIRO, S. 2009. Holocene interdependences of changes in sea surface temperature, productivity and fluvial inputs in the Iberian continental shelf (Tagus mud patch). *Geochemistry, Geophysics, Geosystems*, **10**, Q07U06, <http://dx.doi.org/10.1029/2008GC002367>.
- ROGERSON, M., ROHLING, E.J. & WEAVER, P.P.E. 2006. Promotion of meridional overturning by Mediterranean-derived salt during the last deglaciation. *Paleoceanography*, **21**, PA4101, <http://dx.doi.org/10.1029/2006PA001306>.
- ROGERSON, M., COLMENERO-HIDALGO, E., ET AL. 2010. Enhanced Mediterranean–Atlantic exchange during Atlantic freshening phases. *Geochemistry, Geophysics, Geosystems*, **11**, Q08013, <http://dx.doi.org/10.1029/2009GC002931>.
- ROGERSON, M., ROHLING, E.J., BIGG, G.R. & RAMIREZ, J. 2012. Paleooceanography of the Atlantic–Mediterranean exchange: Overview and first quantitative assessment of climatic forcing. *Reviews of Geophysics*, **50**, RG2003, <http://dx.doi.org/10.1029/2011RG000376>.
- ROHLING, E.J. & COOKE, S. 1999. Stable oxygen and carbon isotopes in foraminiferal carbonate shells. In: SEN GUPTA, B.K. (ed.) *Modern Foraminifera*. Kluwer, Dordrecht, 239–258.
- SALGUEIRO, E., VOELKER, A.H.L., DE ABREU, L., ABRANTES, F., MEGGERS, H. & WEFER, G. 2010. Temperature and productivity changes off the western Iberian margin during the last 150ky. *Quaternary Science Reviews*, **29**, 680–695, <http://dx.doi.org/10.1016/j.quascirev.2009.11.013>.
- SANZ DE GALDEANO, C. & VERA, J.A. 1992. Stratigraphic record and palaeogeographical context of the Neogene basins in the Betic Cordillera, Spain. *Basin Research*, **4**, 21–36, <http://dx.doi.org/10.1111/j.1365-2117.1992.tb00040.x>.
- SARMIENTO, J.L. & TOGGWELLER, J.R. 1984. A new model for the role of the oceans in determining atmospheric  $\text{PCO}_2$ . *Nature*, **308**, 621–626, <http://dx.doi.org/10.1038/308621a0>.
- SCHMIEDL, G. & LEUSCHNER, D.C. 2005. Oxygenation changes in the deep western Arabian Sea during the last 190,000 years: Productivity versus deepwater circulation. *Paleoceanography*, **20**, PA2008, <http://dx.doi.org/10.1029/2004PA001044>.
- SCHMIEDL, G. & MACKENSEN, A. 1997. Late Quaternary paleoproductivity and deep water circulation in the eastern South Atlantic Ocean: Evidence from benthic foraminifera. *Marine Micropaleontology*, **130**, 43–80, [http://dx.doi.org/10.1016/S0031-0182\(96\)00137-X](http://dx.doi.org/10.1016/S0031-0182(96)00137-X).
- SCHMIEDL, G., MACKENSEN, A. & MÜLLER, P.J. 1997. Recent benthic foraminifera from the eastern South Atlantic Ocean: Dependence on food supply and water masses. *Marine Micropaleontology*, **32**, 249–287, [http://dx.doi.org/10.1016/S0377-8398\(97\)00023-6](http://dx.doi.org/10.1016/S0377-8398(97)00023-6).
- SCHMIEDL, G., DE BOVÉE, F., BUSCAIL, R., CHARRIÈRE, B., HEMLEBEN, C., MEDERNACH, L. & PICON, P. 2000. Trophic control of benthic foraminiferal abundance and microhabitat in the bathyal Gulf of Lions, western Mediterranean Sea. *Marine Micropaleontology*, **40**, 167–188, [http://dx.doi.org/10.1016/S0377-8398\(00\)00038-4](http://dx.doi.org/10.1016/S0377-8398(00)00038-4).
- SCHMIEDL, G., MITSCHLE, A., ET AL. 2003. Benthic foraminiferal record of ecosystem variability in the Eastern Mediterranean Sea during times of sapropel S5 and S6 deposition. *Paleogeography, Palaeoclimatology, Palaeoecology*, **190**, 139–164, [http://dx.doi.org/10.1016/S0031-0182\(02\)00603-X](http://dx.doi.org/10.1016/S0031-0182(02)00603-X).
- SCHMIEDL, G., KUHN, T., ET AL. 2010. Climatic forcing of eastern Mediterranean deep-water and benthic ecosystems during the past 22000 years. 704

- 705 *Quaternary Science Reviews*, **29**, 3006–3020, [http://dx.doi.org/10.1016/j.](http://dx.doi.org/10.1016/j.quascirev.2010.07.002)  
 706 quascirev.2010.07.002.
- 707 SCHNEIDER, B. & SCHMITTNER, A. 2006. Simulating the impact of the Panamanian  
 708 seaway closure on ocean circulation, marine productivity and nutrient  
 709 cycling. *Earth and Planetary Science Letters*, **246**, 367–380, [http://dx.doi.](http://dx.doi.org/10.1016/j.epsl.2006.04.028)  
 710 org/10.1016/j.epsl.2006.04.028.
- 711 SCHÖNFELD, J. & ZAHN, R. 2000. Late Glacial to Holocene history of the  
 712 Mediterranean Outflow. Evidence from benthic foraminiferal assem-  
 713 blages and stable isotopes at the Portuguese margin. *Palaeogeography,*  
 714 *Palaeoclimatology, Palaeoecology*, **159**, 85–111, [http://dx.doi.org/10.1016/](http://dx.doi.org/10.1016/S0031-0182(00)00035-3)  
 715 S0031-0182(00)00035-3.
- 716 SIERRO, F.J., GONZÁLEZ-DELGADO, J.A., DABRIO, C.J., FLORES, J.A. & CIVIS, J. 1996.  
 717 Late Neogene depositional sequences in the foreland basin of Guadalquivir  
 718 (SW Spain). In: FRIEND, P. & DABRIO, C.J. (eds) *Tertiary Basins of Spain*.  
 719 Cambridge University Press, Cambridge, 339–345.
- 720 SMYTH, T.J., MILLER, P.I., GROOM, S.B. & LAVENDER, S.J. 2001. Remote sensing  
 721 of sea surface temperature and chlorophyll during Lagrangian experiments  
 722 at the Iberian margin. *Progress in Oceanography*, **51**, 269–281, [http://](http://dx.doi.org/10.1016/S0079-6611(01)00070-2)  
 723 dx.doi.org/10.1016/S0079-6611(01)00070-2.
- 724 THIEDE, J., WINKLER, A., ET AL. 1998. Late Cenozoic history of the polar North  
 725 Atlantic: results from ocean drilling. *Quaternary Science Reviews*, **17**, 185–  
 726 208, [http://dx.doi.org/10.1016/S0277-3791\(97\)00076-0](http://dx.doi.org/10.1016/S0277-3791(97)00076-0).
- 727 TOMCZAK, M. & GODFREY, J.S. 1994. *Regional Oceanography: An Introduction*.  
 728 Pergamon, Oxford.
- 729 VAN DER LAAN, E., SNEL, E., DE KAENEL, E., HILGEN, F.J. & KRIGSMAN, W.  
 730 2006. No major deglaciation across the Miocene–Pliocene boundary: inte-  
 731 grated stratigraphy and astronomical tuning of the Loulja sections (Bou  
 732 Regreg area, NW Morocco). *Paleoceanography*, **21**, PA3011, [http://dx.doi.](http://dx.doi.org/10.1029/2005PA001193)  
 733 org/10.1029/2005PA001193.
- 734 VAN DER LAAN, E., HILGEN, F.J., LOURENS, L.J., DE KAENEL, E., GABOARDI, S. &  
 735 IACCARINO, S. 2012. Astronomical forcing of Northwest African climate and  
 736 glacial history during the late Messinian (6.5–5.5 Ma). *Palaeogeography,*  
 737 *Palaeoclimatology, Palaeoecology*, **313–314**, 107–126, [http://dx.doi.](http://dx.doi.org/10.1016/j.palaeo.2011.10.013)  
 738 org/10.1016/j.palaeo.2011.10.013.
- 739 VAN DER ZWAAN, G.J. & JORISSEN, F.J. 1991. Biofacial patterns in river-  
 740 induced shelf anoxia. In: TYSON, R.V. & PEARSON, T.H. (eds) *Modern and*  
 741 *Ancient Continental Shelf Anoxia*. Geological Society, London, Special  
 742 Publications, **58**, 65–82.
- 743 VERA, J.A. 2000. El Terciario de la Cordillera Bética: estado actual de cono-  
 744 cimientos. *Revista de la Sociedad Geológica de España*, **13**, 345–373.
- 745 VERGNAUD-GRAZZINI, C. 1983. Reconstruction of Mediterranean Late  
 746 Cenozoic hydrography by means of carbon isotope analyses. *Utrecht*  
 747 *Micropaleontological Bulletins*, **30**, 25–47.
- 748 VIDAL, L., BICKERT, T., WEFER, G. & RÖHL, U. 2002. Late Miocene stable iso-  
 749 tope stratigraphy of SE Atlantic ODP Site 1085: relation to Messinian  
 750 events. *Marine Geology*, **180**, 71–85, [http://dx.doi.org/10.1016/S0025-](http://dx.doi.org/10.1016/S0025-3227(01)00206-7)  
 751 3227(01)00206-7.
- 752 VILLANUEVA-GUIMERANS, P. & CANUDO, I. 2008. Assemblages of recent benthic  
 753 foraminifera from the northeastern Gulf of Cádiz. *Geogaceta*, **44**, 139–142.
- 754 VINCENT, E., KILLINGLEY, J.S. & BERGER, W.H. 1980. The magnetic epoch-6  
 755 carbon shift: A change in the ocean's <sup>13</sup>C/<sup>12</sup>C ratio 6.2 million years ago.  
 756 *Marine Micropaleontology*, **5**, 185–203, [http://dx.doi.org/10.1016/0377-](http://dx.doi.org/10.1016/0377-8398(80)90010-9)  
 757 8398(80)90010-9.
- 758 ZAHN, R., SCHÖNFELD, J., KUDRASS, H.R., PARK, M.H., ERLKENKUSER, H. &  
 759 GROOTES, P. 1997. Thermohaline instability in the North Atlantic during  
 760 meltwater events: Stable isotope and ice-rafted detritus records from core  
 761 SO75-26KL, Portuguese margin. *Paleoceanography*, **12**, 696–710, [http://](http://dx.doi.org/10.1029/97PA00581)  
 762 dx.doi.org/10.1029/97PA00581.

Received 26 March 2013; revised typescript accepted 15 November 2013.

Scientific editing by James Hendry.

705  
706  
707  
708  
709  
710  
711  
712  
713  
714  
715  
716  
717  
718  
719  
720  
721  
722  
723  
724  
725  
726  
727  
728  
729  
730  
731  
732  
733  
734  
735  
736  
737  
738  
739  
740  
741  
742  
743  
744  
745  
746  
747  
748  
749  
750  
751  
752  
753  
754  
755  
756  
757  
758  
759  
760  
761  
762  
763  
764  
765  
766  
767  
768